THE JOURNAL OF BIOLOGICAL CHEMISTRY VOL. 287, NO. 11, pp. 8434–8443, March 9, 2012

Structure-Activity Analysis of the Dermcidin-derived Peptide DCD-1L, an Anionic Antimicrobial Peptide Present in Human Sweat*[S]

Received for publication, December 9, 2011, and in revised form, January 17, 2012 Published, JBC Papers in Press, January 18, 2012, DOI 10.1074/jbc.M111.332270

Maren Paulmann[‡], Thomas Arnold[§], Dirk Linke[§], Suat Özdirekcan[§], Annika Kopp[¶], Thomas Gutsmann[¶], Hubert Kalbacher[‖], Ines Wanke[‡], Verena J. Schuenemann[§], Michael Habeck[§], Jochen Bürck[**], Anne S. Ulrich[**], and Birgit Schittek[‡1]

*From the [‡]Department of Dermatology, Eberhard-Karls-University Tübingen, 72076 Tübingen, Germany, the [§]Department of Protein Evolution, Max Planck Institute for Developmental Biology, 72076 Tübingen, Germany, the [¶]Research Center Borstel, Leibniz Center for Medicine and Biosciences, 23845 Borstel, Germany, the [‖]Medical and Natural Sciences Research Center, Eberhard-Karls-University Tübingen, 72074 Tübingen, Germany, and the **Karlsruhe Institute of Technology, Institute for Biological Interfaces (IBG-2) and Institute of Organic Chemistry/CFN, 76344 Eggenstein-Leopoldshafen, Germany*

Background: The anionic DCD-1L is an antimicrobial peptide active in human sweat.
Results: DCD-1L forms cation stabilized oligomeric ion channels.
Conclusion: DCD-1L kills bacteria by forming oligomeric ion channels.
Significance: The anionic antimicrobial peptide DCD-1L is optimally adapted to the conditions in human sweat.

Dermcidin encodes the anionic amphiphilic peptide DCD-1L, which displays a broad spectrum of antimicrobial activity under conditions resembling those in human sweat. Here, we have investigated its mode of antimicrobial activity. We found that DCD-1L interacts preferentially with negatively charged bacterial phospholipids with a helix axis that is aligned flat on a lipid bilayer surface. Upon interaction with lipid bilayers DCD-1L forms oligomeric complexes that are stabilized by Zn^{2+}. DCD-1L is able to form ion channels in the bacterial membrane, and we propose that Zn^{2+}-induced self-assembly of DCD-1L upon interaction with bacterial lipid bilayers is a prerequisite for ion channel formation. These data allow us for the first time to propose a molecular model for the antimicrobial mechanism of a naturally processed human anionic peptide that is active under the harsh conditions present in human sweat.

Antimicrobial peptides (AMPs),[2] also called host-defense peptides, are important effector molecules of the innate immune defense of diverse species protecting epithelial barriers. Several AMPs show a antimicrobial spectrum against a wide range of pathogens including bacteria, fungi, and enveloped viruses (1). The mode of action of most AMPs is not fully understood. The majority of known AMPs are cationic, and there is compelling evidence that electrostatic interactions facilitate the initial binding of the positively charged peptides to the negatively charged bacterial membrane. Additionally, the amphiphilicity of most AMPs promotes their integration into lipid bilayers, leading to membrane disintegration and finally to cell death (2, 3). However, bacteria have developed resistance mechanisms toward cationic AMPs (CAMP), for example by incorporation of positively charged polymers into the cell wall to reduce the net negative charge of the bacterial surface (4).

Anionic antimicrobial peptides (AAMP) are very rare, especially in humans, and it is thought that these peptides were developed in response to the bacterial resistance mechanisms toward CAMPs and have a different mechanism of action (5, 6). Examples of AAMPs are bovine kappacin, the proenkephalin-derived peptides peptide B and enkelytin, maximin H5 from the amphibian *Bombina maxima*, and lysenins from the earthworm *Eisenia fetida* (5, 7–10). It has been suggested that these peptides may synergistically enhance the action of CAMPs or other antimicrobial factors in the first line of defense against microbial infection (11). Furthermore, CAMPs are generally ineffective in body fluids of high salt concentrations, whereas several AAMPs require metal ions or salt for their optimal antimicrobial activity (9, 12). Therefore, it appears that AAMPs complement CAMPs in body locations that are unfavorable for these.

In humans, only a few AAMPs are found, and their mechanism of action is still unclear. Dermcidin (DCD) is one of the best studied human AAMPs. It was discovered by our group as an AMP with no homology to other known AMPs. DCD expression is restricted to human skin, where it is constitutively expressed in eccrine sweat glands, secreted into sweat and transported to the epidermal surface (13). The 110-amino acid

* This work was supported by the Deutsche Forschungsgemeinschaft Grant SFB766.
[S] This article contains supplemental Methods.
[1] To whom correspondence should be addressed: Dept. of Dermatology, Eberhard-Karls-University Tübingen, Liebermeisterstrasse 25, 72074 Tübingen, Germany. Tel.: 49-7071-2980832; Fax: 49-7071-295187; E-mail: birgit.schittek@med.uni-tuebingen.de.
[2] The abbreviations used are: AMP, antimicrobial peptide; AAMP, anionic AMP; AFM, atomic force microscopy; CAMP, cationic AMP; DCD, dermcidin; DDM, dodecyl-β-maltoside; DMPC, 1,2-dimyristoyl-*sn*-glycero-3-phosphocholine; DMPG, 1,2-dimyristoyl-*sn*-glycero-3-phospho-(1′-*rac*-glycerol); DOSY, diffusion-ordered spectroscopy; DPhPC, 1,2-diphytanoyl-*sn*-glycero-3-phosphatidylcholine; LDAO, lauryldimethylamine-oxide; OCD, oriented CD; POPC, 1-palmitoyl-2-oleoyl-*sn*-glycero-3-phosphocholine; POPE, 1-palmitoyl-2-oleoyl-*sn*-glycero-3-phosphoethanolamine; POPG, 1-palmitoyl-2-oleoyl-*sn*-glycero-3-phospho-(1′-*rac*-glycerol); pS, picosiemens; TFE, trifluoroethanol.

precursor is proteolytically processed in sweat, giving rise to several truncated DCD peptides differing in length and charge (14–16). Evidence for a clinical relevance of DCD peptides came from our previous studies indicating that patients with atopic dermatitis have a reduced amount of DCD peptides in sweat which contributed to the high susceptibility of these patients to skin infections and to altered bacterial skin colonization (17).

The most abundant DCD peptide in sweat is the anionic DCD-1L (48-mer, net charge −2), which is able to kill pathogenic microorganisms such as *Staphylococcus aureus*, *Escherichia coli*, *Enterococcus faecalis*, *Staphylococcus epidermidis*, methicillin-resistant *S. aureus*, rifampin- and isoniazid-resistant *Mycobacterium tuberculosis*, *Pseudomonas putida*, *Listeria monocytogenes*, *Salmonella thyphimurium*, and *Candida albicans* (13, 18–20). Remarkably and untypical for an AMP, the antimicrobial activity of DCD-1L is maintained over a broad pH range and at high salt concentrations that resemble the conditions in human sweat (13). This remarkable activity suggested that the functional mechanism of DCD-1L might be different from most other AMPs. Our previous studies showed a binding of DCD-1L to the bacterial surface and an interaction with bacterial membrane phospholipids (6, 21). However, we could not find evidence for membrane permeabilization (21, 22). In this work, we elucidated the mode of antimicrobial action of the anionic DCD-1L by describing (i) the secondary structure and alignment of DCD-1L upon contact with bacterial membrane phospholipids, (ii) the oligomerization tendency of DCD-1L and the influence of cationic divalent ions on self-assembly as well as antimicrobial activity, and (iii) the ability of DCD-1L to form ion channels in planar lipid bilayers. None of these mechanistic aspects has been reported before, and these findings promote a better understanding of a human AAMP in harsh and variable salt conditions as found in sweat.

EXPERIMENTAL PROCEDURES

Bacterial Strain and Peptide—The *S. aureus* strain 113 (ATCC35556) was used in the antimicrobial assay. The bacteria were grown in Luria-Bertani medium at 37 °C and 150 rpm overnight. The culture was then diluted 1:100 in the same medium and bacteria grow to midexponential phase. DCD-1L was purchased from peptide 2.0 (Chantilly, VA) with >95% purity or synthesized utilizing the Fmoc (*N*-(9-fluorenyl)methoxycarbonyl)/tBu chemistry, using the peptide synthesizer Syro II (MultiSynTech, Witten, Germany). After cleavage, the peptide was purified as described previously (21).

CD Spectroscopy—The phospholipids 1,2-diphytanoyl-*sn*-glycero-3-phosphatidylcholine (DPhPC), 1-palmitoyl-2-oleoyl-*sn*-glycero-3-phospho-(1′-*rac*-glycerol) (POPG), 1-palmitoyl-2-oleoyl-*sn*-glycero-3-phosphoethanolamine (POPE) were purchased from Avanti Polar Lipids (Alabaster, AL). POPG and POPE were mixed thoroughly in a glass vial to obtain the POPG/POPE 3:7 (mol/mol) mixture. DCD-1L was added to the phospholipids in a peptide:lipid ratio of 1:50. Chloroform was removed by evaporation under nitrogen and placed under vacuum overnight to remove residual solvent. The peptide/lipid films were resuspended in 50 mM sodium phosphate (pH 6.0) and 20 mM NaCl and vortexed vigorously for the CD measurements. The detergent lauryldimethylamine-oxide (LDAO) or dodecyl-β-maltoside (DDM) was dissolved in water (0.3%). 40 μM DCD-1L was added to the solution and mixed by vortexing. CD spectra of DCD-1L were recorded in a Jasco spectropolarimeter model J-810 (JASCO, Gross-Umstadt, Germany) at 195–250 nm and 25 °C. Ten scans were recorded and averaged at a scanning rate of 200 nm min^{-1}, 2-s response time, and 1-nm bandwidth.

OCD Measurements—The peptide reconstitution into oriented lipid bilayers consisting of POPG, as well as 1,2-dimyristoyl-*sn*-glycero-3-phosphocholine (DMPC) and 1,2-dimyristoyl-*sn*-glycero-3-phospho-(1′-*rac*-glycerol) (DMPG) are described in supplemental Methods.

NMR Sample Preparation and Measurement—NMR samples of 0.5 mM were prepared by drying aliquots of DCD-1L in 2,2,2-trifluoroethanol (Sigma-Aldrich) under nitrogen flow then further dried under vacuum overnight and resuspending in either deionized water containing 10% deuterium oxide (^2H_2O 99.9%; Sigma-Aldrich) or deionized water containing 20–70% deuterated 2,2,2-trifluoroethanol (TFE-$^2H_3$ 99%; Cambridge Isotope Laboratories) resulting in an end volume of 0.5 ml for each sample. Similar samples containing 5 mM $ZnSO_4$ were prepared by dissolving the peptide together with the salt in the corresponding volume of deionized water or deionized water containing 20–70% TFE-$^2H_3$. All NMR spectra were acquired at 298.15 K on a 600-MHz Bruker US Plus Avance III NMR spectrometer equipped with a 5-mm triple-resonance inverse TXI probe (^1H, ^{13}C, ^{15}N) mounted with a *z* axis gradient coil. Data processing and analysis were performed using the Topspin software (Topspin V. 2.1.1; Bruker). The translational diffusion coefficient of DCD-1L was investigated by diffusion-ordered spectroscopy (DOSY-NMR) using standard Bruker-stimulated echo sequences with bipolar gradient pulse pair (24). The stebpgp1s pulse program was used for water diffusion measurements, and stebpgp1s19 that includes a WATERGATE water suppression was used in the case of protein diffusion measurements.

The calibration of B0 field gradient strength, the estimation of the translation diffusion coefficient, and the estimation of the molecular mass are described in detail in supplemental Methods.

Atomic Force Microscopy (AFM)—Exponential phase bacteria (2 ml of *S. aureus* 113, Miller-Luria-Bertani medium) was washed and redissolved in buffer (10 mM Na_2HPO_4 (pH 7.0)) to a final concentration of 6^*10^8 cells/ml. The bacteria were incubated alone (control) or with 62.3 μM DCD-1L at 37 °C for 30 min and were placed on mica afterward. Excess liquid was removed with filter paper, and the bacteria were air-dried at room temperature (21 °C) for 24 h. Dried bacteria were imaged with a MFP-3D atomic force microscope (Asylum Research, Santa Barbara, CA). Imaging in air was performed in contact mode using CSG11-A cantilever ($k = 0.1$ N/m; NT-MDT, Moscow, Russia). The set point was adjusted to guarantee applying minimal forces to the sample. Further image editing (flattening) was done with the MFP-3D software under IGOR Pro (Lake Oswego, OR). Images shown are representative of the overall measurements.

Solid supported bilayers were prepared using vesicle spreading. Briefly, 100 μl of sonicated POPC vesicles (0.1 mg/ml) were added on the freshly cleaved mica. After 30 min, 2 ml of buffer (30 mM Na_2HPO_4, 20 mM NaCl (pH 6.0)) was added. AFM imaging was performed in AC mode using OMCL RC800 PSA cantilevers (Olympus). DCD-1L was added during the experiments to a final concentration of 10 μg/ml.

Single Channel Conductance Measurements—Bilayer membranes were prepared by the painting method as described previously (25). A 1% (w/v) solution of DPhPC in 1:1 (v/v) methanol/chloroform was applied to a 150-μm aperture of the septum of a Teflon cuvette separating both the *cis* and the *trans* compartment. After evaporation of the solvents, the chambers were filled with 1 ml of 1 M KCl, 10 mM MES (pH 6.0). 4 μl of DCD-1L (100 ng/ml) was added to the *cis* chamber, and the solution was shortly stirred. A 1% (w/v) solution of DPhPC in 9:1 *n*-decane/butanol (v/v) was painted across the 150-μm aperture. Single-channel conductance was measured over a range from −100 mV to +100 mV with a pair of Ag/AgCl electrodes to test whether the peptides show directionality. Electrical currents were recorded using a BLM work station (Warner Instruments, Hamden, CT) with a BC-535 amplifier and an LPF-8 Bessel filter connected to an Axon Digidata 1440A digitizer. Data analysis was evaluated with pCLAMP10.0 software (Molecular Devices, Sunnyvale, CA). A minimum of 75 events per measurement was analyzed. Ion selectivity was measured by exchange of 1 M KCl with either 1 M LiCl or 1 M potassium acetate.

Statistical Analysis—Two concurrent models were fit to the conductance measurements and compared with each other. The first model assumes a simple Ohmic relation between voltage and current. The second model accounts for saturation at larger voltages. The first model is a straight line passing through the origin, its slope being the only free parameter. The second model is a hyperbolic tangent describing a sigmoidal curve that is symmetric about the origin; the sigmoid has two free parameters, an amplitude and a scale.

Western Blot Analysis—The influence of lipids on DCD-1L conformation was analyzed by Western blotting (21). The procedure is described in supplemental Methods.

Antimicrobial Assay—Antimicrobial assays were performed using the cfu assay as described previously (22). A culture of *S. aureus* 113 in the exponential phase was harvested, washed twice with the indicated buffer, and suspended in the same buffer. The cells were diluted to a final concentration of 10^6 cfu/ml in buffer. The bacteria were incubated at 37 °C for 2 h with the respective peptide, and a 1:100 dilution of the samples was plated in triplicate on Luria-Bertani agar. After incubation for 20 h at 37 °C the surviving *S. aureus* 113 colonies were counted.

The influence of monovalent or divalent ions on antimicrobial activity of DCD-1L was tested by addition of 10 μM salts (either NaCl, $ZnCl_2$, $MgCl_2$, or $CaCl_2$) to 10.3 μM DCD-1L. Both were incubated for 1 h at 25 °C and then tested against *S. aureus* in 33.3 mM sodium phosphate (pH 6.0) in the cfu assay and as control only against the buffer with the additional salts. In a second step, 4.15 μM DCD-1L was preincubated with 50 μM EDTA for 1 h at 25 °C, tested against the bacteria in 25 mM Tris-HCl (pH 6.5) as well as buffer with EDTA alone. The data shown are the mean values of at least three independent experiments.

RESULTS

Secondary Structure of DCD-1L upon Contact with Membrane Phospholipids—Analysis of the primary structure and physicochemical properties shows that DCD-1L has a net charge of −2 at neutral pH. It consists of 29 polar amino acids (~60%, including Gly) and 19 nonpolar ones (~40%), with several charged residues (7 Lys, 3 Glu, 6 Asp), 1 His, and 8 Gly (Fig. 1*A*). DCD-1L does not contain Cys, Pro, Arg, or any aromatic amino acids. Chou-Fasman predictions suggest three potential α-helical regions and an overall low hydrophobicity. A helical wheel analysis (performed with Heliquest) (26) implies that the hydrophobic amino acids are concentrated on one side of a continuous helix, whereas the charged and hydrophilic amino acids are on the other side. The hydrophobic side contains essentially four types of amino acids (Leu, Ala, Val, Gly) (Fig. 1*A*).

Many CAMPs are known to adopt an α-helical structure upon interaction with bacterial membrane phospholipids or detergents (27). To analyze the secondary structure of DCD-1L and whether it is influenced by these agents in a similar manner, we performed CD spectroscopy using phospholipids with either neutral or negatively charged lipid head groups, resembling those present in eukaryotic and bacterial membranes, respectively.

DCD-1L dissolved in water (Fig. 1*B*) or in buffer (50 mM sodium phosphate (pH 6.0), 20 mM NaCl) (Fig. 1*C*) shows a characteristic minimum at 198 nm, indicating a random coil conformation. Incubation of DCD-1L with the detergents LDAO or DDM, whose micelles are known to mimic a membrane environment, induce an α-helical conformation with spectral minima at 208 nm and 222 nm (Fig. 1*B*). Incubation with the phospholipids DPhPC (zwitterionic), POPG (anionic), or a 7:3 mixture of POPE (zwitterionic)/POPG at a peptide:lipid ratio of 1:50 also induced an α-helical conformation of DCD-1L (Fig. 1*C*). Here, the negatively charged POPG membrane was more effective than DPhPC or POPE/POPG. These observations indicate that interaction of DCD-1L with bacterial membrane phospholipids induces a change in the secondary structure from random coil to an α-helical conformation.

Characterization of DCD-1L in Oriented Lipid Bilayers by OCD—When applied to macroscopically oriented lipid bilayer samples, OCD spectroscopy reveals the alignment of α-helical peptides with respect to the membrane normal (23, 28–32). This method allows us to distinguish clearly different characteristic helix alignments, such as surface-bound, obliquely tilted, or membrane inserted. The relative intensity of the negative "fingerprint" band around 208 nm is directly indicative of the helix tilt angle. When the 208 nm band is more negative than the 222 nm band, it indicates a helix alignment in plane of the lipid layer, whereas zero intensity at 208 nm indicates an upright transmembrane helix.

Because DCD-1L showed the most pronounced α-helical conformation in POPG vesicles (see Fig. 1*C*), the same lipid was used to prepare oriented bilayers at a peptide:lipid ratio of 1:50

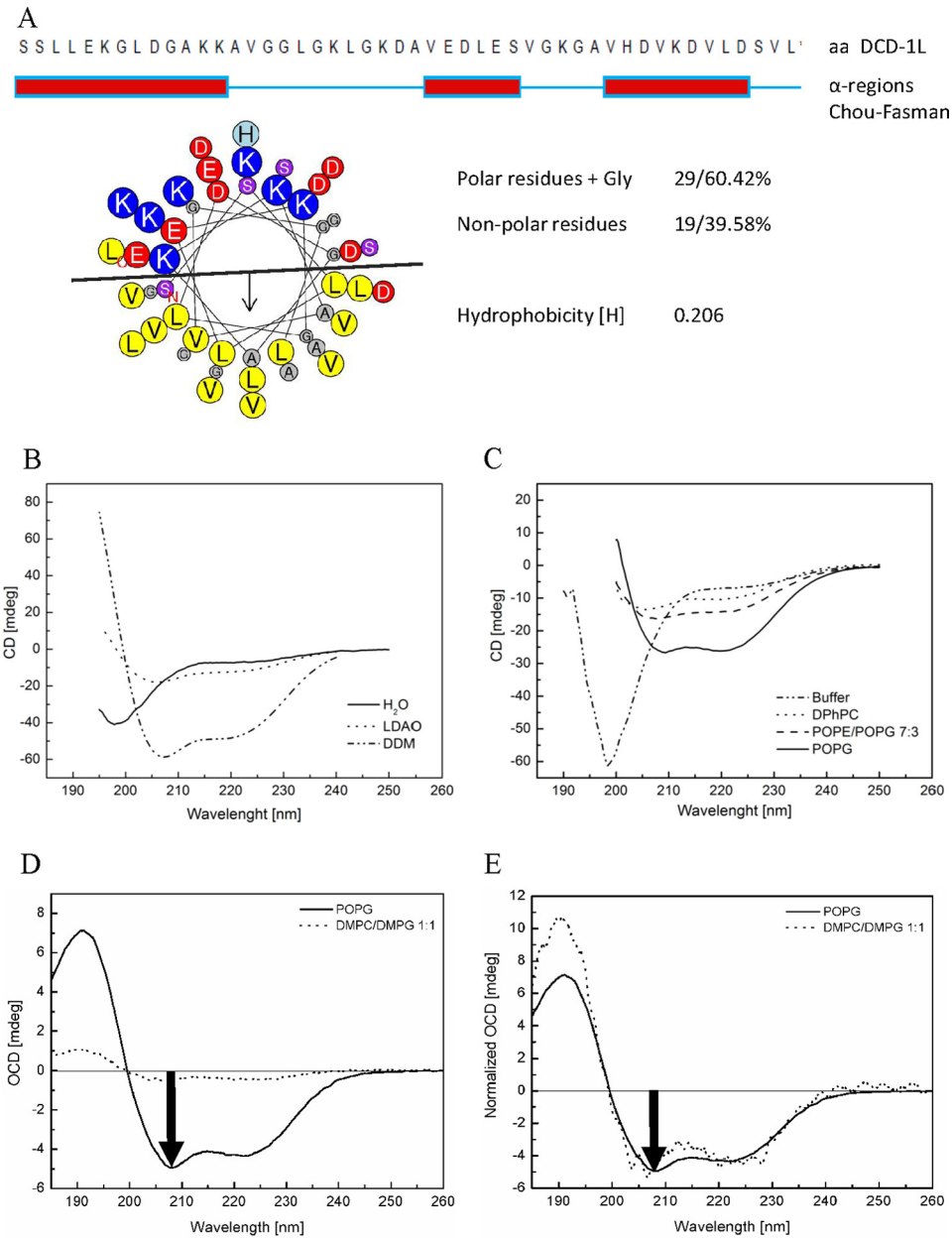

FIGURE 1. **Secondary structure and orientation in bilayers.** *A*, prediction of the secondary structure by the Chou-Fasman algorithm of DCD-1L is based on the amino acid sequence. There are three potential α-helical regions (amino acids 1–13, 26–31, 37–45; 28/48 amino acids (58%)). Prediction analyses by the PSIPRED and JNET algorithms gave similar results, however, with slightly extended α-helical regions (37/48 (77%) and 32/48 (67%), respectively. The helical wheel plot (26) indicates a partitioning into a hydrophilic and a hydrophobic face, as typical for amphiphilic peptides. *B*, CD measurements of DCD-1L in water show an unstructured conformation, which changes into an α-helix in the detergents LDAO or DDM. *C*, CD measurements of DCD-1L in buffer (50 mM sodium phosphate buffer, 20 mM NaCl, pH 6.0) show unstructured conformation, but in the presence of different phospholipid vesicles (DPhPC, POPG, POPE/POPG 7:3), DCD-1L shows that it generally folds as an α-helix in membranes (approximately up to 23%). *D*, oriented CD spectra of DCD-1L in oriented lipid bilayers of POPG and DMPC/DMPG (1:1) reveal an orientation of the amphiphilic helix in the plane of the bilayer. *E*, because there is a lot of scattering due to peptide self-assembly in DMPC/DMPG, the OCD spectra are normalized to the same intensity (at 222 nm) to illustrate the similarity of the line shapes in both lipids.

(mol/mol). The distinct OCD band at 208 nm with a more negative intensity compared with 222 nm clearly shows that DCD-1L is aligned parallel to the membrane surface (Fig. 1*D*). This finding is fully consistent with the expected behavior of a long amphiphilic helix bound to a lipid bilayer. A second OCD sample was prepared with DMPC/DMPG (1:1 mol/mol) because this widely used lipid system has been repeatedly shown to form stable high quality oriented samples with a wide range of different peptides (27). In DMPC/DMPG the OCD spectrum has a much lower intensity than in POPG, despite the same peptide content being present in the two freshly prepared samples. The loss of spectral intensity is attributed to light scattering due to enhanced peptide-peptide interactions, suggesting a tendency of DCD-1L to self-assemble in the membrane. For a better comparison of the two lipid systems, the OCD spectra have been normalized to the same ellipticity value at the minimum around 222 nm (Fig. 1*E*). The very similar line shapes suggest that the peptide has essentially the same helical surface alignment in DMPC/DMPG as in POPG, irrespective of its oligomeric state.

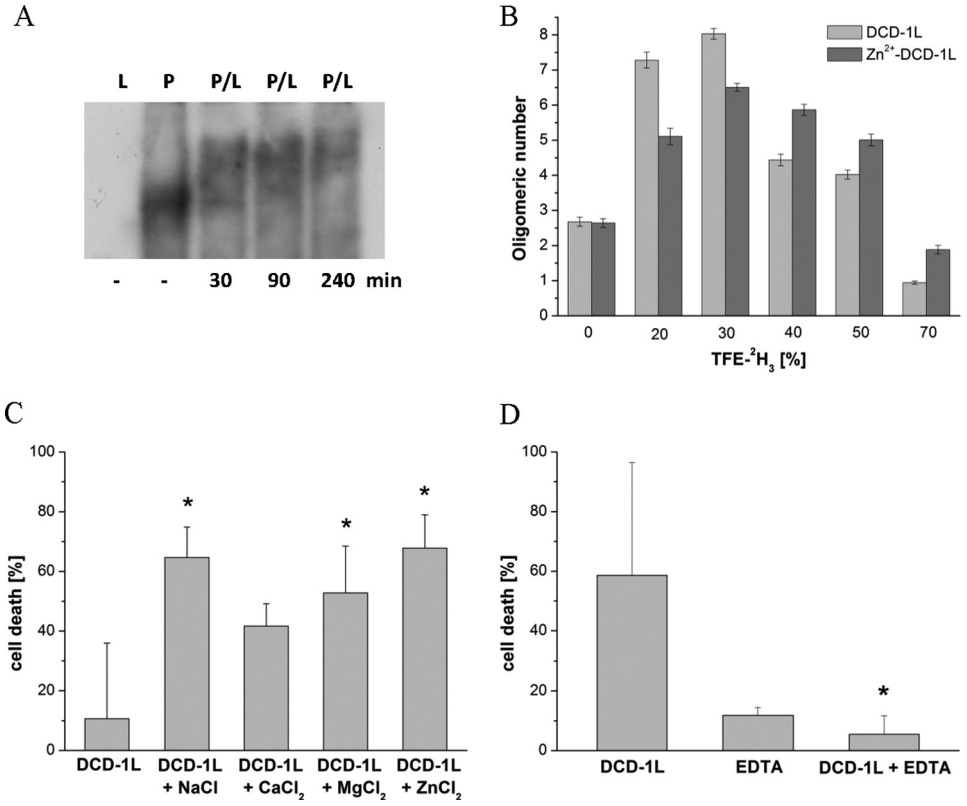

FIGURE 2. **Oligomerization and ions increase antimicrobial activity of DCD-1L.** *A*, Western blot analysis of a native PAGE indicates an oligomerization of DCD-1L in POPG vesicles (phospholipid (*L*), POPG; peptide (*P*), DCD-1L; *P/L*, 1:50). *B*, DOSY-NMR of DCD-1L with or without $ZnSO_4$ is shown as is the extent of oligomerization before and after the addition of increasing concentrations of TFE-$^2H_3$. *Error bars* reflect the S.D. obtained per sample. The S.D. were obtained from the analysis of 8–13 different peaks per sample. Outliers were discarded after applying robust statistics analysis, and peaks that could not be fitted to a single exponential decay were not included in further analysis. *C*, addition of different ions (10 μM) increased the antimicrobial activity of DCD-1L (10.3 μM) against *S. aureus* 113. Buffer: 33.3 mM sodium phosphate (pH 6.0). *, $p < 0.05$. *D*, in contrast, after cation depletion by addition of 50 μM EDTA, the antimicrobial activity against *S. aureus* 113 was lost. Buffer: 25 mM Tris-HCl (pH 6.5), DCD-1L (4.15 μM). *, $p < 0.05$.

Structure-Function Relationship of Antimicrobial Activity—DCD-1L is known to oligomerize (21), it binds to bacterial membrane phospholipids (6), and our OCD results have implied that oligomerization can also take place in membranes (see Fig. 1*D*). Therefore, we examined directly whether bacterial membrane phospholipids influence oligomerization of DCD-1L as a function of time. As illustrated in Fig. 2*A*, binding of DCD-1L (peptide, P) to POPG (phospholipid, L) induces a time-dependent oligomerization of the peptide. Furthermore, DOSY-NMR of DCD-1L in increasing concentrations of the membrane-mimetic solvent TFE-$^2H_3$ indicates oligomerization of the peptide (Fig. 2*B*). Because divalent cations can stabilize bacterial membranes by forming ion bridges to the phosphate groups of phospholipids (33), we analyzed the effect of the divalent cation Zn^{2+} on the oligomerization behavior of DCD-1L in the structure-inducing solvent TFE. We incubated DCD-1L with increasing percentages of TFE-$^2H_3$ and analyzed in each of these samples the influence of TFE with or without Zn^{2+} on the extent of oligomerization (Fig. 2*B*). Addition of up to 30% TFE increased the extent of DCD-1L self-assembly, which was slightly more pronounced for peptides in the absence of Zn^{2+}. At TFE concentrations above 30%, oligomerization decreases again, but interestingly a higher degree of self-assembly is maintained in the presence of Zn^{2+}. Thus, at higher TFE concentrations, the presence of Zn^{2+} appears to stabilize the oligomeric state of DCD-1L.

The anionic DCD-1L is highly bactericidal against the Gram-positive pathogen *S. aureus* 113 (22). We noticed that addition of divalent (Zn^{2+}, Ca^{2+}, Mg^{2+}) and monovalent (Na^+) ions enhances the antimicrobial activity of DCD-1L against *S. aureus* 113 significantly (Fig. 2*C*). In line with these results, depletion of divalent ions by the addition of EDTA resulted in the loss of antimicrobial activity of DCD-1L (Fig. 2*D*). Our data suggest that not only the environment of a bacterial membrane but also divalent ions such as Zn^{2+} affect the extent of oligomerization and that this correlates with the antimicrobial activity.

DCD-1L Changes Bacterial Surface Morphology and Induces a Destabilization of Lipid Bilayers—AFM was used to visualize the morphological changes in the cell envelope upon interaction with DCD-1L. Typical images of untreated *S. aureus* are presented in Fig. 3, *A* and *B*, with a conglomerate of several bacterial colonies surrounded by slime or extracellular matrix components. The close up view displays single *S. aureus* with a size of ~1 μm^2 with a smooth, unruptured surface (Fig. 3*B*). DCD-1L-treated bacteria showed a strong modification of the surface topography and the surrounding matrix and an increase in the surface roughness of *S. aureus* with a number of bleb-like structures (Fig. 3, *C* and *D*). In addition, the surrounding extracellular matrix changed from a smooth, regular type to a grained type. These changes of the bacterial cell surface mor-

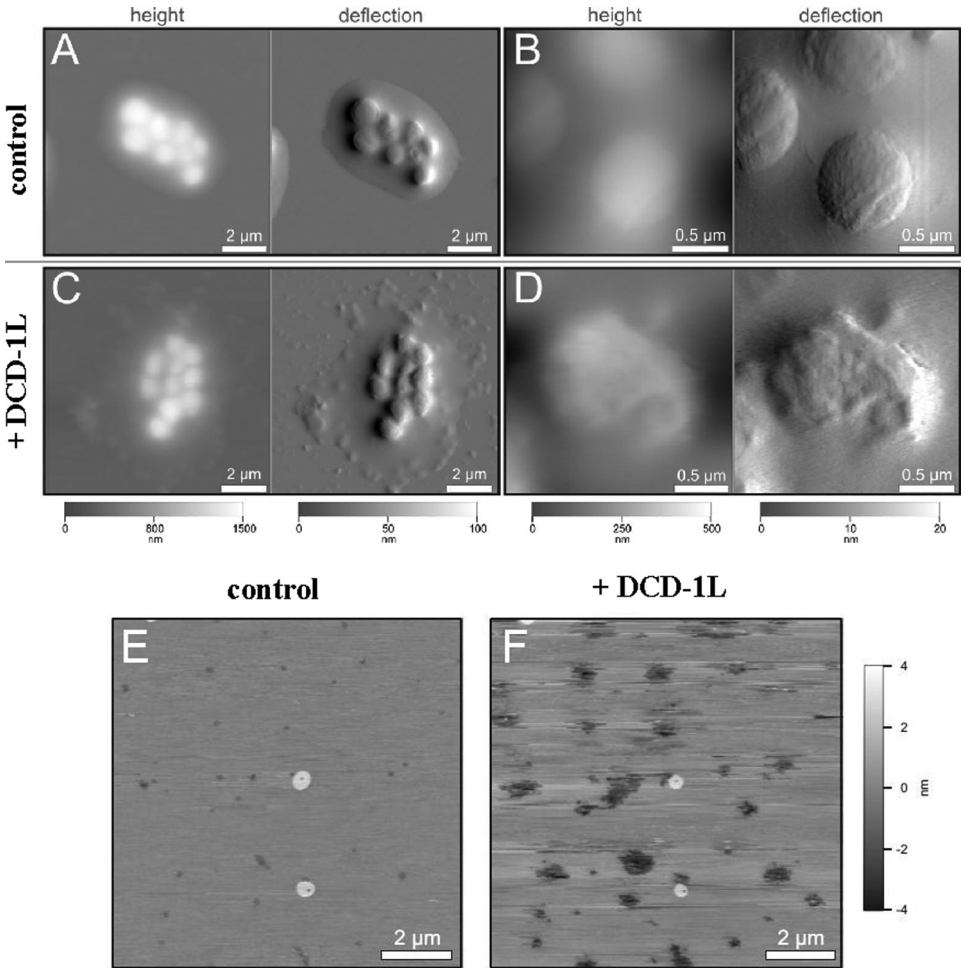

FIGURE 3. **AFM images of DCD-1L-treated bacteria.** AFM images of height (*left*) and deflection (*right*) are bundled for measurements, each of which was performed in contact mode in air. *A*, untreated *S. aureus* 113 as control. *B*, higher resolution of the untreated bacteria. *C*, DCD-1L (62.3 μM)-treated *S. aureus* 113. *D*, higher resolution of the treated bacteria. *E*, image of solid supported lipid bilayers composed of POPC without DCD-1L imaged in buffer in AC mode at room temperature. The height images of one position are shown. *F*, image of POPC bilayers with DCD-1L measured in buffer in AC mode at room temperature.

phology suggest that DCD-1L interferes with the bacterial membrane stability (34, 35). Indeed, AFM images of membrane phospholipids (POPC) incubated with DCD-1L showed a destabilization of the lipid bilayer (Fig. 3, *E* and *F*). The images clearly show the appearance of defects within the lipid bilayer after addition of DCD-1L. These defects might be induced solely by the peptides or by the force applied by the cantilever tip. However, they were only observed in case of peptide-treated membranes.

DCD-1L Forms Ion Channels in Lipid Bilayer—Pore formation in bacterial membranes is a very common mechanism of antimicrobial peptides and proteins. We thus examined the pore forming properties of DCD-1L with single-channel conductance measurements in DPhPC black lipid bilayers. The results clearly show that DCD-1L is very potent in ion channel formation after an initial reconstitution, which takes several minutes. An example for a recording at 50 mV is illustrated in Fig. 4*A*, showing the initial reconstitution of a peptide channel in the black lipid bilayer. Once inserted into the membrane, the current increases stepwise until the membrane finally breaks. The insertion of the first channel appears to trigger subsequent insertions and suggests a self-enhancing, cooperative mechanism of pore formation. We then studied whether the conductance measurements are better explained by the Ohmic model or by the sigmoidal model. Fig. 4*B* shows the models obtained by fitting all data. The estimated slope of the linear model is 0.029 pA mV^{-1}. The estimated scale and amplitude of the sigmoid are 0.028 mV^{-1} and 2.14 pA. The sigmoidal is clearly preferred over the Ohmic model. The sum of absolute deviations S is significantly smaller for the sigmoid ($S = 1384$) than for the Ohmic model ($S = 1558$) and the Bayesian information criterion (BIC) also shows that the sigmoidal model (BIC = 2782) is preferred over the Ohmic model (BIC = 3123). Consequently, the channel conductance of DCD-1L shows a voltage-dependent decline (Fig. 4*C*). The highest conductance was observed at membrane potentials of 10 mV (98 pS) and −10 mV (151 pS). With increasing voltages (up to 100 mV and −100 mV), the conductance decreased to ~20 pS to 30 pS, indicating that only a limited number of ions can cross the channel per time. These observations are in agreement with the previously observed slow kinetics of the membrane potential breakdown, and consequently, killing of the bacteria by DCD-1L (22).

To test for possible ion selectivity, we performed conductance measurements with other electrolytes than KCl. As shown in Fig. 4*D*, the average conductance in 1 M KCl is ~60 pS at 20 mV. The replacement of potassium or chloride with large and

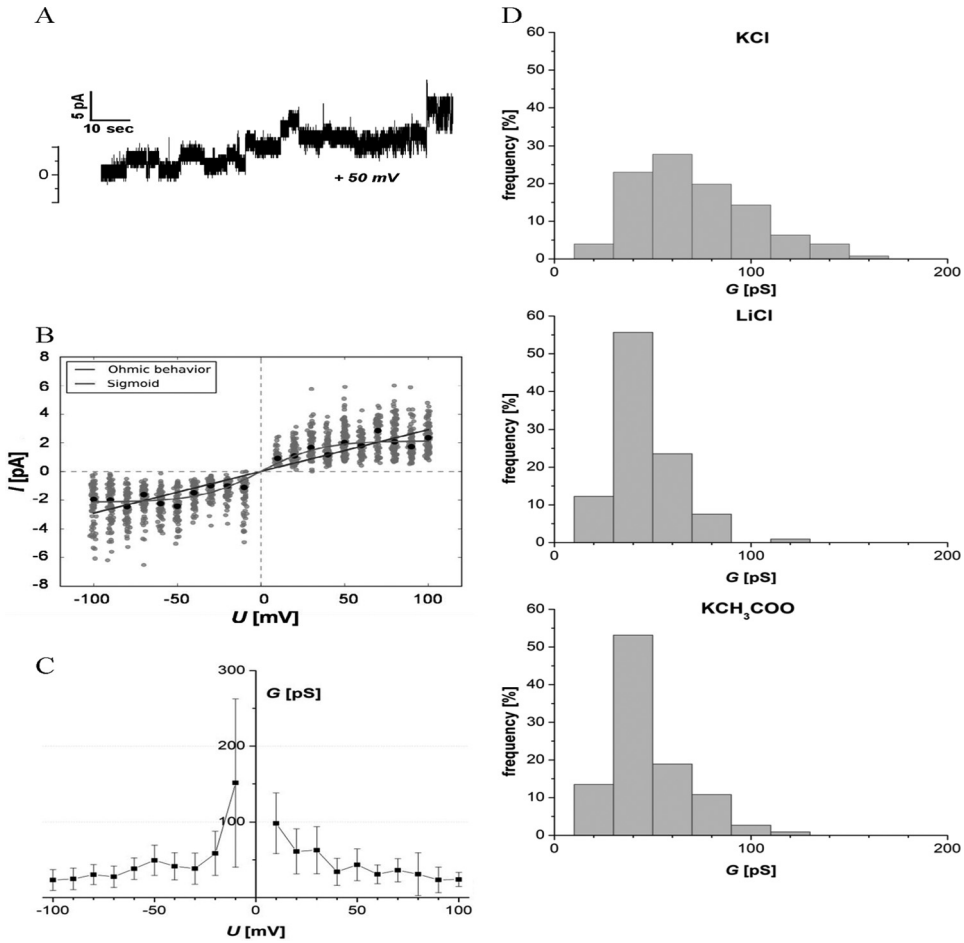

FIGURE 4. **Electrophysiological characterization of DCD-1L.** A, representative current trace of DCD-1L at 50 mV showing an initial channel insertion followed by others leading to a stepwise increase of the current. *B*, evaluation of DCD-1L single-channel conductance in DPhPC black lipid bilayers. Measurements were carried out with 1 M KCl, 10 mM MES (pH 6.0), and 400 pg/ml DCD-1L; at least 75 insertion events per voltage were evaluated. Shown are the fitted models obtained with all data (*blue*, Ohmic model; *green*, sigmoid). The *gray dots* are the raw measurements (random noise was added to the × values for better visibility of the data which otherwise fall onto *vertical lines*). *Black dots* indicate the median of the measurements at each voltage. *C*, voltage-dependent decline of the channel conductance of DCD-1L. An increase in voltages leads to a saturation of conductance at 20–30 pS. *D*, histograms of measured single-channel conductances observed for DCD-1L, measured at 20 mV using different electrolytes. The average conductance of at least 75 reconstitution events was 60 pS in 1 M KCl and was reduced to 40 pS in 1 M LiCl or potassium acetate, respectively.

less mobile ions (lithium cations or acetate anions) resulted in a decreased channel conductance (40 pS) which is highly significant ($p < 0.001$). Due to the comparable conductance in either LiCl or potassium acetate, we conclude that the DCD-1L channel is neither anion- nor cation-selective.

DISCUSSION

In this study, we show that the anionic dermcidin-derived peptide DCD-1L, present in human eccrine sweat, adopts an α-helical structure upon interaction with bacterial membrane phospholipids and can form ion channels in black lipid bilayers. Western blotting, OCD, and DOSY-NMR analyses indicate that DCD-1L has a tendency to oligomerize and that this assembly is promoted by Zn^{2+} and/or a membrane-mimetic environment. Furthermore, Zn^{2+} and other divalent cations are found to enhance the antimicrobial activity of DCD-1L.

Single channel conductance analyses with planar lipid bilayers showed that DCD-1L can form ion channels in membranes. The conductance behavior indicated that only a comparably low number of ions can pass the channel, which is in good agreement with the observed slow kinetics of changes in the bacterial membrane potential and killing of the bacteria (22). In our previous experiments, using electron microscopy or propidium iodide staining of the bacteria, we could not detect pore formation in the bacterial membrane (21, 22). Based on the new electrophysiological data, especially the saturation of the pore conductance at only slightly elevated voltages and the decrease of conductance using bigger ions, it appears that the pores formed by DCD-1L are too small to be detected using electron microscopy or staining methods. Comparison of the conductance with typical values measured for known cationic pore-forming peptides (like magainin-1, Pep5, NP-1, melittin) suggests that the DCD-1L channel size is probably in the range or even beneath that of these peptides (36–39). We have no evidence that the ion channel is anion- or cation-selective because we did not observe differences in conductance when using different electrolytes. This finding contrasts the properties of ion channels formed by other AMPs. For example, cationic magainin-1 from *Xenopus laevis* forms anion-selective channels in patch-clamped lipid bilayers with defined conductances

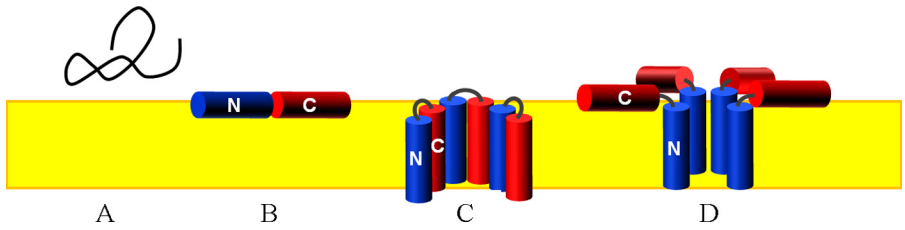

FIGURE 5. **Functional model for the mechanism of antimicrobial activity of DCD-1L.** *A*, anionic DCD-1L is unstructured in aqueous solution according to CD and NMR. *B*, upon binding to a bacterial membrane the peptide folds into an amphiphilic α-helix, which is aligned parallel to the membrane surface according to OCD. DCD-1L can self-assemble into higher order oligomers according to DOSY-NMR and OCD, and it can form ion channels according to electrophysiological analysis. However, when the 48-mer peptide is folded as a helix, it is twice as long as the thickness of a lipid bilayer. *C*, we thus propose that the monomer could fold into a helical hairpin that would perfectly match the membrane thickness and neutralize most charges. *D*, alternatively, the cationic N terminus might participate in a toroidal pore. Self-assembly in either form would support the formation of transmembrane ion channels, which would lead to bacterial cell death.

of 366 pS and 683 pS (36). Binding of magainin-1 to phospholipid vesicles, where the peptide self-assembles, inserts, and form largely pentameric pores, induces the leakage of cellular material. We speculate that *in vivo*, the channel formed by DCD-1L functions as a proton channel as suggested for kappacin, an AAMP from bovine milk (9, 10). For kappacin it has been proposed that it forms ion channels with a proton influx at acidic pH, which slowly results in bacterial cell death by reducing intracellular pH (9).

DCD-1L is an amphiphilic peptide with a cationic N-terminal region (amino acids 1–23) and an anionic C-terminal part (amino acids 24–48). The net charge at neutral pH is −2 and becomes less charged under acidic conditions (pI = 5.07). Cationic peptides are known to bind to the anionic bacterial surface by electrostatic interactions, which facilitates their entry into the bacterial cell or results in pore formation and finally in bacterial death. The net negative charge of DCD-1L renders an attachment of the peptide via electrostatic interactions difficult. We presume that the cationic N-terminal part is mainly responsible for the binding of DCD-1L to the bacterial surface and to the negatively charged bacterial phospholipids. This view was recently proposed by Jung *et al.* who used liquid state NMR to solve the structure of DCD-1L in 50% TFE and to characterize its interaction with phospholipid vesicles (40).

The analysis of transposon mutants of *S. aureus* showed that DCD-1L interacts directly with the phospholipids in the bacterial membrane (6). In the present study, we demonstrate by CD spectroscopy that DCD-1L adopts an α-helical structure preferentially in the presence of anionic POPG compared with zwitterionic phospholipids. OCD indicates that the α-helix binds parallel to the plane of the lipid bilayer. A flat alignment of the DCD-1L helix within the membrane surface is perfectly compatible with the amphiphilic structure of the monomer. Such binding has also been described for many helical CAMPs that form a carpet on the membrane surface at low concentrations (23).

OCD also showed that phospholipids can promote self-assembly of DCD-1L, supporting previous observations of oligomeric complexes *in vitro* and *in vivo* in human sweat, although without previously analyzing the factors influencing oligomerization (21). The DOSY-NMR analyses clearly indicate that the membrane-mimetic solvent TFE favors oligomer formation. Complex formation of DCD-1L is increased up to a TFE concentration of 30%, whereas at higher TFE concentrations complex formation is reduced again. In the comparatively hydrophilic environment of ≤30% TFE, we may speculate that this helix-promoting solvent induces the formation of amphiphilic helices that would cluster together via their hydrophobic faces. At higher TFE concentrations, the complexes can disperse again as they become better soluble in the more hydrophobic environment. Interestingly, at high TFE levels, the presence of Zn^{2+} tends to promote the self-assembly, presumably via the hydrophilic face of the amphiphilic helices. These findings suggest that DCD-1L oligomer formation is influenced by the general environmental conditions (hydrophobicity, pH, concentration of salt and divalent ions), as well as by the local peptide concentration when bound to a lipid membrane.

It is known that the pH has an effect on solubility and self-association of peptides, as shown for clavanins (41). Acidic pH seems functionally similar to Zn^{2+} because it increases the positive charge on peptides with basic amino acids as histidines, arginines, or lysines. It has been shown that this leads to enhanced antimicrobial activity of histidine-rich peptides (42). Likewise, metal ions such as Zn^{2+} could increase the interaction of DCD-1L with the bacterial surface by forming peptide-lipid salt bridging as described for other AAMPs as kappacin or surfactant-anionic peptides (SAAPs) (9). Alternatively, the divalent metal ions could also promote the self-assembly of DCD-1L by forming peptide-peptide salt bridges via histidine, aspartate, or glutamate side chains. In any case, the harsh conditions in eccrine sweat with an acidic pH (pH 5–6.5) and several mono- and divalent ions seem to optimally promote the interaction of monomeric DCD-1L with bacterial membranes. Our data imply that self-assembly of DCD-1L can lead to the formation of ion channels, with a diameter similar to or even smaller than the barrel-stave model of CAMPs (43). Several studies have previously shown that peptide self-assembly in the membrane-bound state correlates with antimicrobial activity (30), whereas complex formation in an aqueous environment had no effect on antimicrobial activity (44).

Taking all of our data together, we may propose a functional model for the mechanism of antimicrobial activity of DCD-1L. The peptide is initially unstructured and presumably monomeric when secreted in human sweat (Fig. 5*A*). In the presence of a negatively charged bacterial surface, the cationic N terminus probably gets attracted electrostatically, such that DCD-1L binds to the membrane surface as an amphiphilic α-helix (Fig. 5*B*). Upon interaction with the bacterial membrane it self-as-

sembled into a higher oligomeric state as a function of time. Structurally, the most intriguing aspect in the case of DCD-1L oligomerization is the fact that the 48-mer peptide has a length of >7 nm when folded as a continuous α-helix. This helix is twice as long as the thickness of a typical membrane with only about 3 nm. A transmembrane insertion as a continuous helix, as one may simplistically envisage, would thus imply that half of the molecule sticks out of the membrane, which is unreasonable. It is also unlikely that a full-length helix would span the membrane with an obliquely tilted angle. We thus propose two possible scenarios for the functionally active state of membrane-bound DCD-1L. In analogy to other CAMPs, Fig. 5*C* illustrates that the cationic N terminus might be able to fold back onto its anionic C-terminal region to form an intramolecular hairpin, in which most charges are compensated. Alternatively, Fig. 5*D* suggests that the cationic N-terminal region of DCD-1L might form a toroidal pore across the lipid bilayer, while the amphiphilic C terminus remains floating on the membrane surface. The secondary structure prediction of DCD-1L as well as the experimental NMR structure in 50% TFE (40) had shown an intrinsically flexible amphiphilic structure with three distinct α-helical regions, which would readily allow a sharp turn in the middle of the sequence. By forming either an intramolecular helical hairpin (Fig. 5*C*) or a kinked structure (Fig. 5*D*), the resulting DCD-1L bundle would have the perfect height to span the bacterial membrane. Nevertheless, the two functional models are based on speculation and still need to be confirmed and/or rejected experimentally by solid-state NMR and site-directed mutagenesis in the α-helical regions. Our OCD analysis has so far shown only a surface alignment of DCD-1L under equilibrium conditions. It may be a challenge to trap the proposed membrane-immersed form for structural analysis, as it might only be present as a transient state or in the presence of a transmembrane voltage. Nevertheless, the present study has provided unambiguous evidence for a membrane-perturbing function of DCD-1L, an unusually long anionic peptide that is ideally adapted to the acidic and salty conditions in human sweat to fulfill its role in host defense.

REFERENCES

1. Zasloff, M. (2002) Antimicrobial peptides of multicellular organisms. *Nature* **415,** 389–395
2. Dennison, S. R., Wallace, J., Harris, F., and Phoenix, D. A. (2005) Amphiphilic α-helical antimicrobial peptides and their structure/function relationships. *Protein Pept. Lett.* **12,** 31–39
3. Zelezetsky, I., and Tossi, A. (2006) α-Helical antimicrobial peptides: using a sequence template to guide structure-activity relationship studies. *Biochim. Biophys. Acta* **1758,** 1436–1449
4. Peschel, A., and Sahl, H. G. (2006) The co-evolution of host cationic antimicrobial peptides and microbial resistance. *Nat. Rev. Microbiol.* **4,** 529–536
5. Lai, R., Liu, H., Hui Lee, W., and Zhang, Y. (2002) An anionic antimicrobial peptide from toad *Bombina maxima*. *Biochem. Biophys. Res. Commun.* **295,** 796–799
6. Li, M., Rigby, K., Lai, Y., Nair, V., Peschel, A., Schittek, B., and Otto, M. (2009) *Staphylococcus aureus* mutant screen reveals interaction of the human antimicrobial peptide dermcidin with membrane phospholipids. *Antimicrob. Agents Chemother.* **53,** 4200–4210
7. Bruhn, H., Winkelmann, J., Andersen, C., Andrä, J., and Leippe, M. (2006) Dissection of the mechanisms of cytolytic and antibacterial activity of lysenin, a defence protein of the annelid *Eisenia fetida*. *Dev. Comp. Immunol.* **30,** 597–606
8. Goumon, Y., Lugardon, K., Kieffer, B., Lefèvre, J. F., Van Dorsselaer, A., Aunis, D., and Metz-Boutigue, M. H. (1998) Characterization of antibacterial COOH-terminal proenkephalin-A-derived peptides (PEAP) in infectious fluids: importance of enkelytin, the antibacterial PEAP209-237 secreted by stimulated chromaffin cells. *J. Biol. Chem.* **273,** 29847–29856
9. Harris, F., Dennison, S. R., and Phoenix, D. A. (2009) Anionic antimicrobial peptides from eukaryotic organisms. *Curr. Protein Pept. Sci.* **10,** 585–606
10. Malkoski, M., Dashper, S. G., O'Brien-Simpson, N. M., Talbo, G. H., Macris, M., Cross, K. J., and Reynolds, E. C. (2001) Kappacin, a novel antibacterial peptide from bovine milk. *Antimicrob. Agents Chemother.* **45,** 2309–2315
11. Harris, F., Dennison, S. R., and Phoenix, D. A. (2011) Anionic antimicrobial peptides from eukaryotic organisms and their mechanisms of action. *Curr. Chem. Biol.* **5,** 142–153
12. Jenssen, H., Hamill, P., and Hancock, R. E. (2006) Peptide antimicrobial agents. *Clin. Microbiol. Rev.* **19,** 491–511
13. Schittek, B., Hipfel, R., Sauer, B., Bauer, J., Kalbacher, H., Stevanovic, S., Schirle, M., Schroeder, K., Blin, N., Meier, F., Rassner, G., and Garbe, C. (2001) Dermcidin: a novel human antibiotic peptide secreted by sweat glands. *Nat. Immunol.* **2,** 1133–1137
14. Baechle, D., Flad, T., Cansier, A., Steffen, H., Schittek, B., Tolson, J., Herrmann, T., Dihazi, H., Beck, A., Mueller, G. A., Mueller, M., Stevanovic, S., Garbe, C., Mueller, C. A., and Kalbacher, H. (2006) Cathepsin D is present in human eccrine sweat and involved in the postsecretory processing of the antimicrobial peptide DCD-1L. *J. Biol. Chem.* **281,** 5406–5415
15. Flad, T., Bogumil, R., Tolson, J., Schittek, B., Garbe, C., Deeg, M., Mueller, C. A., and Kalbacher, H. (2002) Detection of dermcidin-derived peptides in sweat by ProteinChip technology. *J. Immunol. Methods* **270,** 53–62
16. Rieg, S., Seeber, S., Steffen, H., Humeny, A., Kalbacher, H., Stevanovic, S., Kimura, A., Garbe, C., and Schittek, B. (2006) Generation of multiple stable dermcidin-derived antimicrobial peptides in sweat of different body sites. *J. Invest. Dermatol.* **126,** 354–365
17. Rieg, S., Steffen, H., Seeber, S., Humeny, A., Kalbacher, H., Dietz, K., Garbe, C., and Schittek, B. (2005) Deficiency of dermcidin-derived antimicrobial peptides in sweat of patients with atopic dermatitis correlates with an impaired innate defense of human skin *in vivo*. *J. Immunol.* **174,** 8003–8010
18. Cipáková, I., Gasperík, J., and Hostinová, E. (2006) Expression and purification of human antimicrobial peptide, dermcidin, in *Escherichia coli*. *Protein Expression Purification* **45,** 269–274
19. Lai, Y. P., Peng, Y. F., Zuo, Y., Li, J., Huang, J., Wang, L. F., and Wu, Z. R. (2005) Functional and structural characterization of recombinant dermcidin-1L, a human antimicrobial peptide. *Biochem. Biophys. Res. Commun.* **328,** 243–250
20. Vuong, C., Voyich, J. M., Fischer, E. R., Braughton, K. R., Whitney, A. R., DeLeo, F. R., and Otto, M. (2004) Polysaccharide intercellular adhesin (PIA) protects *Staphylococcus epidermidis* against major components of the human innate immune system. *Cell. Microbiol.* **6,** 269–275
21. Steffen, H., Rieg, S., Wiedemann, I., Kalbacher, H., Deeg, M., Sahl, H. G., Peschel, A., Götz, F., Garbe, C., and Schittek, B. (2006) Naturally processed dermcidin-derived peptides do not permeabilize bacterial membranes and kill microorganisms irrespective of their charge. *Antimicrob. Agents Chemother.* **50,** 2608–2620
22. Senyürek, I., Paulmann, M., Sinnberg, T., Kalbacher, H., Deeg, M., Gutsmann, T., Hermes, M., Kohler, T., Götz, F., Wolz, C., Peschel, A., and Schittek, B. (2009) Dermcidin-derived peptides show a different mode of action than the cathelicidin LL-37 against *Staphylococcus aureus*. *Antimicrob. Agents Chemother.* **53,** 2499–2509
23. Bürck, J., Roth, S., Wadhwani, P., Afonin, S., Kanithasen, N., Strandberg, E., and Ulrich, A. S. (2008) Conformation and membrane orientation of amphiphilic helical peptides by oriented circular dichroism. *Biophysl. J.* **95,** 3872–3881
24. Johnson C. S., Jr. (1999) Diffusion ordered nuclear magnetic resonance spectroscopy: principles and applications. *Progress NMR Spectrosc.* **34,** 203–256

25. Arnold, T., Poynor, M., Nussberger, S., Lupas, A. N., and Linke, D. (2007) Gene duplication of the eight-stranded β-barrel OmpX produces a functional pore: a scenario for the evolution of transmembrane β-barrels. *J. Mol. Biol.* **366,** 1174–1184
26. Gautier, R., Douguet, D., Antonny, B., and Drin, G. (2008) HELIQUEST: a web server to screen sequences with specific α-helical properties. *Bioinformatics* **24,** 2101–2102
27. Grage, S. L., Afonin, S., and Ulrich, A. S. (2010) Dynamic transitions of membrane-active peptides. *Methods Mol. Biol.* **618,** 183–207
28. Chen, F. Y., Lee, M. T., and Huang, H. W. (2002) Sigmoidal concentration dependence of antimicrobial peptide activities: a case study on alamethicin. *Biophys. J.* **82,** 908–914
29. Lange, C., Müller, S. D., Walther, T. H., Bürck, J., and Ulrich, A. S. (2007) Structure analysis of the protein translocating channel TatA in membranes using a multiconstruct approach. *Biochim. Biophys. Acta* **1768,** 2627–2634
30. Olah, G. A., and Huang, H. W. (1988) Circular dichroism of oriented α helices. I. Proof of the exciton theory. *J. Chem. Phys.* **89,** 2531–2538
31. Windisch, D., Hoffmann, S., Afonin, S., Vollmer, S., Benamira, S., Langer, B., Bürck, J., Muhle-Goll, C., and Ulrich, A. S. (2010) Structural role of the conserved cysteines in the dimerization of the viral transmembrane oncoprotein E5. *Biophys. J.* **99,** 1764–1772
32. Wu, Y., Huang, H. W., and Olah, G. A. (1990) Method of oriented circular dichroism. *Biophys. J.* **57,** 797–806
33. Puskin, J. S. (1977) Divalent cation binding to phospholipids: an EPR study. *J. Membr. Biol.* **35,** 39–55
34. Hartmann, M., Berditsch, M., Hawecker, J., Ardakani, M. F., Gerthsen, D., and Ulrich, A. S. (2010) Damage of the bacterial cell envelope by antimicrobial peptides gramicidin S and PGLa as revealed by transmission and scanning electron microscopy. *Antimicrob. Agents Chemother.* **54,** 3132–3142
35. Hammer, M. U., Brauser, A., Olak, C., Brezesinski, G., Goldmann, T., Gutsmann, T., and Andrä, J. (2010) Lipopolysaccharide interaction is decisive for the activity of the antimicrobial peptide NK-2 against *Escherichia coli* and *Proteus mirabilis*. *Biochem. J.* **427,** 477–488
36. Duclohier, H., Molle, G., and Spach, G. (1989) Antimicrobial peptide magainin I from *Xenopus* skin forms anion-permeable channels in planar lipid bilayers. *Biophys. J.* **56,** 1017–1021
37. Kagan, B. L., Selsted, M. E., Ganz, T., and Lehrer, R. I. (1990) Antimicrobial defensin peptides form voltage-dependent ion-permeable channels in planar lipid bilayer membranes. *Proc. Natl. Acad. Sci. U.S.A.* **87,** 210–214
38. Kordel, M., Benz, R., and Sahl, H. G. (1988) Mode of action of the staphylococcinlike peptide Pep 5: voltage-dependent depolarization of bacterial and artificial membranes. *J. Bacteriol.* **170,** 84–88
39. Tosteson, M. T., and Tosteson, D. C. (1981) The sting: melittin forms channels in lipid bilayers. *Biophys. J.* **36,** 109–116
40. Jung, H. H., Yang, S. T., Sim, J. Y., Lee, S., Lee, J. Y., Kim, H. H., Shin, S. Y., and Kim, J. I. (2010) Analysis of the solution structure of the human antibiotic peptide dermcidin and its interaction with phospholipid vesicles. *BMB Rep.* **43,** 362–368
41. Lee, I. H., Cho, Y., and Lehrer, R. I. (1997) Effects of pH and salinity on the antimicrobial properties of clavanins. *Infect. Immun.* **65,** 2898–2903
42. Kacprzyk, L., Rydengård, V., Mörgelin, M., Davoudi, M., Pasupuleti, M., Malmsten, M., and Schmidtchen, A. (2007) Antimicrobial activity of histidine-rich peptides is dependent on acidic conditions. *Biochim. Biophys. Acta* **1768,** 2667–2680
43. Afonin, S., Grage, S. L., Ieronimo, M., Wadhwani, P., and Ulrich, A. S. (2008) Temperature-dependent transmembrane insertion of the amphiphilic peptide PGLa in lipid bilayers observed by solid state 19F NMR spectroscopy. *J. Am. Chem. Soc.* **130,** 16512–16514
44. Chen, Y., Guarnieri, M. T., Vasil, A. I., Vasil, M. L., Mant, C. T., and Hodges, R. S. (2007) Role of peptide hydrophobicity in the mechanism of action of α-helical antimicrobial peptides. *Antimicrob. Agents Chemother.* **51,** 1398–1406